Review

Supramolecular Nanomachines as Stimuli-Responsive Gatekeepers on Mesoporous Silica Nanoparticles for Antibiotic and Cancer Drug Delivery

Chi-An Cheng[1,3], Tian Deng[2,3], Fang-Chu Lin[2,3], Yao Cai[2,3], Jeffrey I. Zink[2,3]✉

1. † Department of Bioengineering, University of California Los Angeles, Los Angeles, California 90095, United States
2. # Department of Chemistry & Biochemistry, University of California Los Angeles, Los Angeles, California 90095, United States
3. § California NanoSystems Institute, University of California Los Angeles, Los Angeles, California 90095, United States

✉ Corresponding author: zink@chem.ucla.edu

Abstract

Major objectives in nanomedicine and nanotherapy include the ability to trap therapeutic molecules inside of nano-carriers, carry therapeutics to the site of the disease with no leakage, release high local concentrations of drug, release only on demand – either autonomous or external, and kill the cancer cells or an infectious organism. This review will focus on mesoporous silica nanoparticle carriers (MSN) with a large internal pore volume suitable for carrying anticancer and antibiotic drugs, and supramolecular components that function as caps that can both trap and release the drugs on-command.

Caps that are especially relevant to this review are rotaxanes and pseudorotaxanes that consist of a long chain-like molecule threaded through a cyclic molecule. Under certain conditions discussed throughout this review, the cyclic molecule can be attracted to one end of the rotaxane and in the presence of a stimulus can slide to the other end. When the thread is attached near the pore opening on MSNs, the sliding cyclic molecule can block the pore when it is near the particle or open it when it slides away.

The design, synthesis and operation of supramolecular systems that act as stimuli-responsive pore capping devices that trap and release molecules for therapeutic or imaging applications are discussed. Uncapping can either be irreversible because the cap comes off, or reversible when the cyclic molecule is prevented from sliding off by a steric barrier. In the latter case the amount of cargo released (the dose) can be controlled. These nanomachines act as valves.

Examples of supramolecular systems stimulated by chemical signals (pH, redox, enzymes, antibodies) or by external physical signals (light, heat, magnetism, ultrasound) are presented. Many of the systems have been studied *in vitro* proving that they are taken up by cancer cells and release drugs and kill the cells when stimulated. Some have been studied in mouse models; after IV injection they shrink tumors or kill intracellular pathogens after stimulation. Supramolecular constructs offer fascinating, highly controllable and biologically compatible platforms for drug delivery.

Key words: Rotaxane, pseudorotaxane, supramolecular, mesoporous silica nanoparticles, drug delivery

Introduction

Supramolecular constructs on mesoporous silica nanoparticles (MSNs) for drug delivery, the subject of this review, resulted from the convergence of two fields: sol-gel synthesis of metal oxide solids [1], and organic syntheses of supramolecular rotaxanes and pseudorotaxanes [2]. The primary current goal is to use porous sol-gel nanomaterials to carry cargo molecules such as drugs, and supramolecular

constructs to hold the cargo in place until stimulated to release it on command. Success in this venture would result in the decrease in off-target effects of the drugs by carrying them with no leakage to the site of the disease, and releasing high local concentrations of them where and when desired.

Sol-gel chemistry had a resurgence in popularity a decade ago because it is a solution-based synthesis for making metal oxide solids. Silica (silicon dioxide) was one of the favorites because of its optical transparency, the ability to synthesize the glass around organic and biomolecules (including enzymes) [3–6], the ability to use molds to make monoliths in desired shapes, and the ability to synthesize films [7–9] fibers and nanoparticles in amazing varieties of shapes and sizes.

Especially interesting was the syntheses of glass around liquid crystalline phases of surfactant molecules to template mesoporous glass. After the hydrolysis and condensation of the precursor molecules tetraalkoxysilanes around rod-shaped two-dimensional hexagonal phases of cetyltammonium chloride, the templating surfactant was removed by solvent extraction or calcination to make silica materials with uniform sized and well-ordered pores. This procedure was patented and the material named MCM-41 even though the same material had been patented 16 years earlier [10] and rediscovered prior to the second patent. Further research led to controllable synthesis of nanospheres. Typical MSNs discussed in this review are spheres about 100 nm in diameter with tubular pores about 2.5 nm in diameter. The size of supramolecular nanomachines should be comparable to that of the pores of MSNs in order to trap the cargo inside. The majority of supramolecular nanomachines discussed in this article are capable of capping pores of this size (2.5 nm). The biocompatibility of these materials has been reviewed [11,12] and many examples of *in vitro* and *in vivo* studies are shown in this review (Tables 1 and 2). One gram of particles has a surface area of about 1000 m^2 and a pore volume of about 1 cm^3. Because typical anticancer drugs have a density of about 1g/cm^3, the carrying capacity can be 100 wt% (although this upper limit is rarely achieved because of imperfect molecular packing).
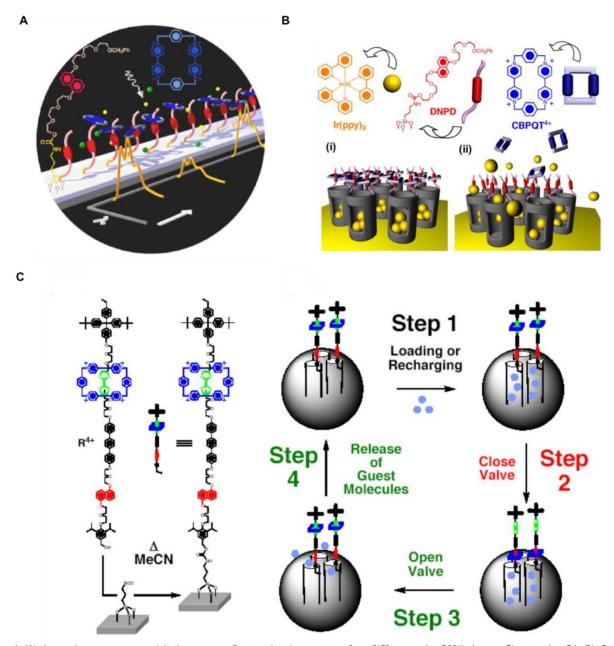
During the same period, supramolecular organic molecule-based structures were being synthesized. Especially relevant to this review are the now famous rotaxanes consisting of a long chain-like molecule threaded through a cyclic molecule (known as a pseudo-rotaxane) [2]. When large "blocking" molecules were attached to the ends of the chain, the cyclic molecule could not slide off and was held in place by "mechanical bonds". Under certain conditions discussed throughout this review, the cyclic molecule could be attracted to one end of the rotaxane and in the presence of a stimulus could slide to the other end. The bonding of one end of this organic structure to mesoporous sol-gel glass was the key to unlock and open the door to an amazing variety of drug-delivery vehicles.

The ground-breaking paper that reported the system is shown in Figure 1A [13]. A thread containing a dioxynaphthalene was attached to a silica surface and a cyclic ring molecule containing two bipyridinium units was threaded on to it. Chemical reduction of the ring weakened the attraction to the thread thus releasing the ring. Oxidation caused it to re-attach, and the threading/dethreading was monitored by the quenching and reappearance of the naphthalene fluorescence. This rotaxane system worked on the solid support.

The next advance was the attachment of the organic component to the regions around the pore openings on silica particles (Figure 1B) [14]. Ir(PPY)$_3$ was chosen as the cargo molecule because it is brightly fluorescent and stable in the presence of the oxidizing and reducing agents required to trigger the trapping and release. When the paraquat was attracted to the dioxynapthalene near the pore opening, the cargo molecules were trapped in the pore. When the reducing agent CNBH$_3^-$ was added, the pseudorotaxane disassembled releasing the fluorophore into the solution. The fluorescence of the naphthalene component that had been partially quenched by the paraquat increased in intensity. This supramolecular nanovalve is an example of a molecular machine consisting of a solid framework with movable parts capable of doing work.

Continuing studies further refined and enhanced the new nanomachine. A more complicated stalk containing two different binding sites for the paraquat enabled the system to be switched back and forth as a result of sequential oxidation and reduction steps (Figure 1C) [15]. One end of the stalk was attached to the pore openings on the silica and a bulky group was attached on the other end to prevent escape of the ring. This rotaxane was the first example of a truly reversible nanovalve. The positioning of the rotaxane on the particle was refined [16] and the system was reconfigured such that it could be stimulated by light energy via a photoredox transducers [17,18].

The focus of these pioneering studies was to prove that the rotaxane actually moved when attached to a silica surface, and then to prove that it could actually trap molecules in pores and release them on command. When it became clear that the

supramolecular concept of a controllable cap on a pore was a reality, attention turned to potential applications. A challenging one was to improve on nanomaterials as drug delivery vehicles. Liposomes were being used, but drug release from them was not controllable. Rotaxane caps are, but they only operated in non-aqueous media. Attentions turned to water-based supramolecular systems and the results of those investigations, including operation *in vitro* and *in vivo*, are described in this review and summarized in Table 1 and 2, respectively.

Figure 1 (A) A pseudorotaxane on a solid silica support. Reprinted with permission from [13], copyright (2001) Angew. Chemie - Int. Ed. (B) Graphical representations of operation of nanovalves gating the pore openings on silica particles. (i) The orifices of the nanopores (diameter 2 nm) are covered with pseudorotaxanes (formed between DNPD and CBPQT4+) which trap the luminescent Ir(ppy)₃ molecules inside the nanopores. (ii) Upon their reduction, the CBPQT2+ bisradical dications are released and allow the Ir(ppy)₃ to escape. Reprinted with permission from [14], copyright (2004) J. Am. Chem. Soc. (C) Graphical representations of the surface attachment of bistable rotaxanes to silica particles along with a cycle for loading and release of guest molecules. Left: The structural formula of the bistable [2]rotaxane R4+ and the procedure used for tethering R4+ to the surface of mesoporous silica particles. Right: The proposed mechanism for the operation of the nanovalve. The moving part of the molecular valve is a CBPQT4+ ring (blue), which shuttles between a TTF station (green) and a DNP station (red) under redox control. The openings of the cylindrical pores on the silica are blocked by the CBPQT4+ ring when the valve is closed. Guest molecules (turquoise spheres) are loaded in Step 1 by diffusion into the open pores when the CBPQT4+ ring is located on the TTF station. The valve is closed in Step 2 by oxidation of the TTF unit to its dication, causing the CBPQT4+ ring to move to the DNP station, which is much closer to the openings of the pores. The valve can be opened (Step 3) by adding ascorbic acid to reduce the TTF dication back to its neutral state, whereupon the CBPQT4+ ring moves back from the DNP station to be relocated around the much more π electron-rich TTF station, releasing the guest molecules in Step 4. The valve is ready for recharging (*i.e.*, returning to Step 1). Thus, the valve can be closed and opened reversibly. The silica particles are not drawn to scale, and only a few of the ordered pores are shown. Reprinted from [15], copyright (2005) Proc. Natl. Acad. Sci.

Table 1. Cell lines used in studies with supramolecular nanomachines

Cell line	Description	Drug delivered	Reference
MDA-MB-231	human breast cancer cells	doxorubicin	25
MiaPaCa-2	human pancreatic cancer cells	doxorubicin	34
THP-1 and KB-31	THP-1: human differentiated leukemia monocytes KB-31: human squamous carcinoma cells	doxorubicin	36
MDM and THP-1	MDM: human monocyte-derived macrophages THP-1: human differentiated leukemia monocytes (macrophage-like cells)	moxifloxacin	37
L929	murine aneuploidy fibrosarcoma cells	N/A	52
A549	adenocarcinomic human alveolar basal epithelial cells	doxorubicin	53
PANC-1	human pancreatic cancer cells	doxorubicin	62
HeLa and COS7	HeLa: human cervical cancer cells COS7: African green monkey SV40-transformed kidney fibroblast cells	doxorubicin	66

Table 2. Animal models used in studies with supramolecular nanomachines

Animal model	Description	Drug delivered	References
mice	MiaPaCa-2 xenografts	doxorubicin	34
mice	*Francisella tularensis* infection	moxifloxacin	37

Supramolecular nanovalves for stimuli responsive cargo delivery

Macrocyclic molecules such as cucurbit[n]urils (n=5-10, CB[n]), cyclodextrins (CDs), crown ethers, and pillararenes tend to form inclusion complexes with guests and can be dissociated reversibly or irreversibly in response to external stimuli in aqueous solution. Therefore, these families of polymacrocycles have been used as the biologically friendly rings on the nanovalves for drug delivery applications [19]. In this section, two categories of supramolecular capping systems will be discussed based on their reversibility of capping and uncapping. First, pseudorotaxane nanovalves are discussed. In the closed position the cyclic molecules are on a binding site on the stalks that is close to the pore openings. Upon activation they slide away from and off of the stalk. The system is reusable because the cyclic molecules can be rethreaded, but they are irreversible because in biological conditions the cyclic molecules diffuse away from the particles and have such low concentrations that the rate of rebinding is very low. Next, reversible rotaxane nanovalves are discussed. These nanovalves, in contrast, are reversible because a bulky group at the end of the stalk prevents the cyclic molecules from leaving the stalk. At the end of this section, we will also describe "inactive supramolecular systems". Different from the pseudorotaxane and rotaxane nanovalves, the active parts of this inactive system are not the supramolecular inclusion complexes, but bond breaking between the bulky inclusion complexes and the nanoparticles occurs.

Irreversible pseudorotaxane based nanovalves

Cucurbit[n]urils

CB[n] are pumpkin-shaped cyclic methylene-bridged glycoluril oligomers that were named cucurbituril because of their resemblance to pumpkins, the most prominent member of the *cucurbitaceae* plant family [20,21]. CB[n] analogues have a common depth (9.1 Å), but their widths and volumes vary. Their shape of the narrower portals to the entry with the wider cavity produces significant steric barriers to guest association and dissociation [22]. To have biological applications, water solubility is an essential property. The three members of the cucurbiturils CB[5], CB[6], and CB[7] possess modest solubility in water. Among these CB[n] analogues, CB[6] was the first and the most widely studied cucurbituril, with greater than a one hundred year history.

CB[6] rings and bisammonium stalks

Angelos *et al.* synthesized pseudorotaxanes consisting of CB[6] rings and bisammonium stalks bonded to MSNs (Figure 2) [23]. Alkyne-functionalized MSNs were synthesized and the particles were loaded with rhodamine B (RhB) cargo molecules by soaking the MSNs in a RhB solution (0.5 mM) for 5 h at room temperature. Then an excess of CB[6] was added to the above mixture and thus capping the pore. The release of RhB was carried out by raising the pH. The binding of CB[6] with the bisammonium stalks is pH-dependent; at neutral and acidic pH the CB[6] rings encircle the stalks tightly and thus block the pores. At basic pH, deprotonation of the stalks switch off the ion-dipole interactions

between the CB[6] rings and the stalks resulting in dethreading of CB[6]. The subsequent release of the RhB cargo was monitored as a function of time by fluorescence spectroscopy.
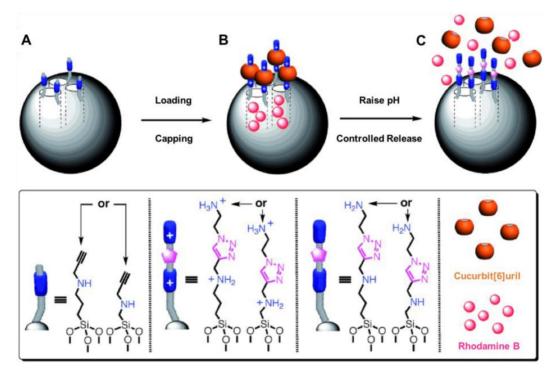
CB[6] rings and dialkyl-4,4-bipyridinium (viologen) stalks

Khashab *et al.* designed another pH-controlled CB[6]-based pseudorotaxane nanoparticle system [24]. In this case, dialkyl-4,4-bipyridinium (viologen) dicationic guests form highly stable inclusion complexes with CB[6] hosts, giving rise to a well-known [2]pseudorotaxane (Figure 3). The internal cavity of CB[6] forms strong complexes with the alkyl chains in the stalk by means of hydrophobic interactions and electrostatic interactions between the

positive charge on viologen and carbonyl oxygens on CB[6]. Under acidic conditions (pH 4), the carboxylate end group becomes protonated attracting the CB[6] macrocycle away from the pore towards the end of the stalk and thus releases the cargo.

CB[6] rings and N-(6-aminohexyl) aminomethyltriethoxysilane stalks

The CB[6] valve can be stimulated by means other than pH. Thomas *et al.* expanded the use of CB[6] by constructing a thermal-sensitive nanovalve that is operable by oscillating magnetic fields (OMFs) (Figure 4) [25]. This system was also the first study exploring the possibility of OMF-triggered cargo release. The carrier, a core-shell nanoparticle with a superparamagnetic iron oxide core and a mesoporous

Figure 2. The alkyne-functionalized MSNs MCM-41 are loaded (A→B) with rhodamine B (RhB) molecules, and capped (A→B) with CB[6] during the CB[6]-catalyzed alkyne-azide 1,3-dipolar cycloadditions. RhB molecules are released (B→C) by switching off the ion–dipole interactions between the CB[6] rings and the bisammonium stalks by raising the pH and deprotonating the amines. Reprinted with permission from [23], copyright (2008) Angew. Chemie - Int. Ed.
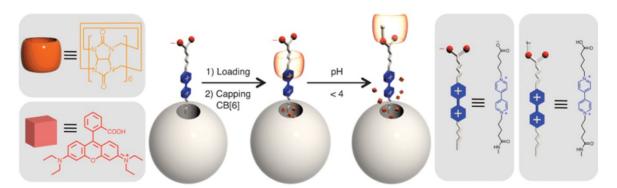

Figure 3. Design and preparation of viologen threads (stalk component) and CB[6] (cap) on MSNs that operate under pH-control. Reprinted with permission from [24], copyright (2009) Chem. Commun.

silica shell, was synthesized by phase-transferring the iron oxide nanoparticle into the water phase and forming an outer silica shell. The resulted core-shell MSN was then grafted with N-(6-aminohexyl) aminomethyltriethoxysilane (stalk) by refluxing the nanoparticles with the stalks in toluene overnight. RhB and doxorubicin (DOX) were used as the cargos. The loading of the cargo was done by soaking the stalk-mechanized core-shell MSNs in RhB or DOX solution overnight. Finally, the cargo-loaded nanoparticles were capped with CB[6] rings and the whole system was ready to use. The hydrophobic cavity of CB[6] encircles the alkyl chain of the stalk through non-covalent London force, ion-dipole interactions and hydrogen bonding. The binding constant between CB[6] ring and the stalk decrease at high temperature, thus slipping off the cap and allowing the cargo to diffuse out. The authors not only demonstrated the release of RhB and DOX under OMFs, but they also showed that internal heat generated from the iron oxide core and not bulk heating actuated the CB[6]/stalk pseudorotaxane complex.

The thermal-sensitive valve-controlled particles were taken up by MDA-MB-231 breast cancer cells and released DOX on-command in the cells. After being taken up by the cells, the mechanized nanoparticles showed minimal DOX release. Upon exposure to OMFs, the local heating generated from the superparamagnetic core initiated the release of DOX from the silica pores and induced cell apoptosis.

Croissant *et al.* demonstrated that this thermal-sensitive nanovalve was operable by plasmonic heating (Figure 5) [26]. The authors developed a novel one-pot method to synthesize the carrier, a core/shell structure with a 20 nm gold core and a 150 nm mesoporous silica shell (designated as Au@MSN). In this method, the authors used autoreduction of tetrachloroaurate ions in the presence of cetyltrimethylammonium bromide (CTAB), which is the template of mesopore formation. The Au@MSNs were mechanized with the stalks, loaded with RhB cargos, and finally capped with CB[6] rings. The nanovalves were activated through the localized heat generated from plasmonic heating of the Au core. Similar to the magnetic heating, the local temperature rise is useful for spatially controlled drug delivery.
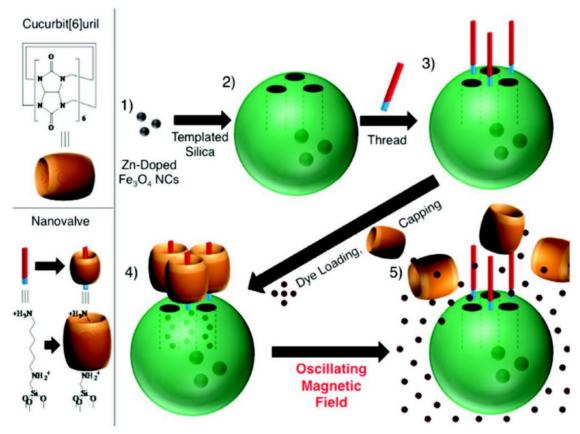

Figure 4. Scheme of the synthesis of the mechanized nanoparticles and their operation under oscillating magnetic fields (OMFs). (1) Supraparamagnetic nanoparticles are synthetically positioned at the core of MSNs; (2) the molecular machine is then attached to the nanoparticle's surface; (3) the drug is loaded into the particle and (4) the pores are capped to complete the system. (5) Drug release is realized using remote heating via an OMF. Reprinted with permission from [25], copyright (2010) J. Am. Chem. Soc.
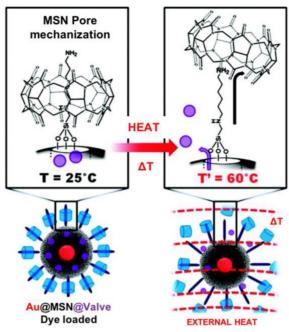
Figure 5. External heating of a suspension of Au@MSN@Valve to 60 °C causes dissociation of the CB[6] caps from the stalks and release of the cargo molecules from the pores. Reprinted with permission from [26], copyright (2012) J. Am. Chem. Soc.

CB[7] rings and cinnamamide stalks

Another CB[n] analogue, CB[7], was found to possess a suitable cavity and form stable host-guest complexes with trans-cinnamamide derivatives [20,27,28]. This CB[7]-cinnamamide complex is responsive to UV light (300 nm) [29]. After UV irradiation, a trans- to cis- conformational change of cinnamamide is induced, leading to dissociation caused by a change in the steric hindrance. Utilizing this property, CB[7]-cinnamamide pseudorotaxane has been developed as a light-switchable supramolecular nanovalve on MSNs [30]. The outer surface of the MSNs was first functionalized with 3-aminopropyl groups. Amino modified nanoparticles were reacted with cinnamoyl chloride, and then the pores of the functionalized MSNs were loaded with RhB. Finally, pores were capped with CB[7], which forms stable inclusion complexes with the grafted cinnamamide moieties. The authors showed that 300 nm UV light induced the release of the entrapped RhB due to the trans- to cis-conformational change of cinnamamide which dethreaded the inclusion complex. The authors also showed that by using pulsed UV irradiation, a "ladder" controlled-release profile of RhB could be achieved, which could potentially control the dose of the released drugs for further applications.

Cyclodextrins

α-CD rings and anilinoalkane stalks

Alpha cyclodextrin (α-CD) molecules have been

shown to have strong binding for benzene and benzene derivatives. The binding affinity between α-CD and the anilinoalkane group decreases after protonation of the aniline when the pH is lowered causing dissociation to occur. Du and coworkers [31] designed a pH-responsive nanovalve based on α-CD and anilinoalkane stalks on hollow MSNs (Figure 6). Three different linkers were attached on the particles' surfaces and the cargo, fluorescent Hoechst 33342, was loaded into pores. α-CD was added to MSN as the capping agent. To optimize the length of the linker control of the pore openings, N-phenylaminomethyltriethoxysilane (PhAMTES) and N-phenylaminopropyltrimethoxysilane (PhAPTMS) were both tested. The amine group on PhAMTES was one carbon from silica, whereas that of PhAPTMS was three carbons away. To tune the trigger pH that opened the nanovalves, p-anisidine with higher pKa than that of aniline was linked to 3-iodopropyltrimethoxysiliane (IPTMS) and used as the third linker. The release profiles of the three nanovalves were obtained by monitoring the emission intensity of cargos in aqueous solution after acidification. The trigger pH is governed by the pKa of aniline nitrogen: the release profiles of the three nanovalves were similar if triggered by pH 3.5 or 5, but only the nanovalve with IPTMS can be triggered at biorelevant pH 6. This nanovalve was an early example of a pH controlled pseudorotaxane nanovalve system in aqueous solution, and the study systematically explored the effects of stalk length and pH conditions on the cargo release profiles.
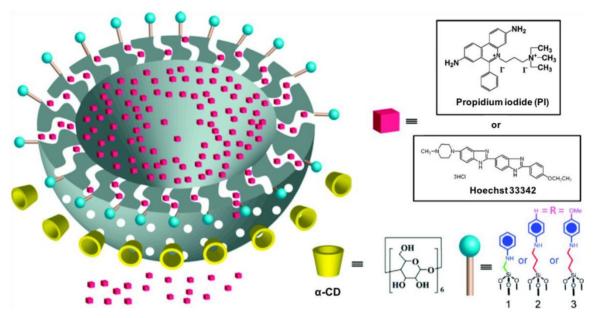
Figure 6. Depiction of a cross section of a hollow nanoparticle illustrating the wormlike pores connecting the interior to the surrounding solution. The stalks and the α-CD rings that control the pore openings are also shown. Reprinted with permission from [31], copyright (2009) J. Am. Chem. Soc.
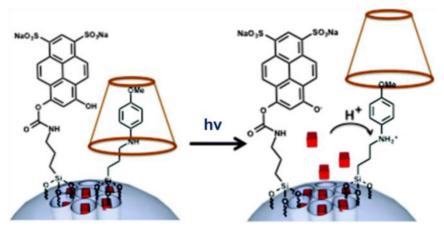

Figure 7. Light activation of a pH nanovalve. A photoacid is attached adjacent to an acid-stimulated aniline/α-CD valve. Photoexcitation of the photoacid causes protonation of the stalk and releases the cap and cargo. Reprinted with permission from [33], copyright (2014) Chem. Commun.

Dong and coworkers [32] studied the effects of polymer coatings around MSNs on the aniline based pseudorotaxane nanovalves' properties. Surface coatings of low molecular weight polyethylene imine (PEI) carry and protect siRNA, and it was of interest to determine if the nanovalves would function properly for drug delivery underneath such a coating. For the initial study, 1.8 kDa PEI was coated by electrostatic interaction and hydrogen bonding on 120 nm MSNs with pH sensitive nanovalves that open at pH 3.5. The second model consists of polyethylene imine-polyethylene glycol (PEI-PEG)-coated 50 nm MSNs. The release profiles of fully assembled MSNs with both polymer coating and nanovalves were similar to those of MSNs with only nanovalves, which indicated that the polymer coating did not stop cargo release.

Guardado-Alvarez and coworkers [33] reported a light responsive nanovalve based on α-CD on a stalk containing an aniline derivative and a photoacid, 6,8-dihydroxy-1,3-pyrenedisulfonic acid (Figure 7). The latter was covalently bonded to an MSN's surface next to a pH responsive nanovalve, and when it was photoexcited at 408 nm, it transferred protons to adjacent stalks. Protonation of the aniline nitrogen caused the α-CD to dissociate due to decreased binding affinity. Propidium iodide (PI) was used as the cargo and was monitored by fluorescence intensity excited at 448 nm. The release profile showed that there was little premature release at neutral pH, and an increase in florescence intensity in solution after irradiation. The pH of the bulk solution stayed neutral but the local pH on MSN surface became acidic. No release was observed when the

solution surrounding the MSN was buffered at pH 8 because the buffer prevented acidification. In addition, no release was observed when the system was irradiated at 514 nm, a wavelength that was not absorbed by the photoacid. By turning on and off the pump laser, the amount of release was controllable.

Hwang *et al.* further refined the pH-responsive aniline/α-CD inclusion complex toward *in vitro* and *in vivo* applications by attaching a targeting protein, transferrin (Tf), to the surface of the particle (Figure 8) [34]. It was important to determine if the valve would still operate under a protein coating and if the system would actively target receptors on cancer cells. The authors put fluorescent imaging molecules in the pores and targeting proteins and pH-sensitive aniline/α-CD nanovalves on the same MSN. At neutral pH, the pseudorotaxane was stable and able to seal cargo inside the pores of MSNs. However, the binding constant between the stalk and α-CD decreased when the phenyl amine was protonated (pKa ≈ 6) in acidic environment, and thus dethreaded the α-CD and released the cargo. Because transferrin was also bonded onto the nanoparticles, the authors first optimized the relative surface coverages of the nanovalves and transferrin in order be able to deliver the maximum amount of cargo controlled by the valves and also obtain the maximum amount of cell targeting with the transferrin. Dox was used as the anticancer drug for both *in vitro* and *in vivo* studies.

In vitro testing with human pancreatic cancer cells (MiaPaCa-2) showed an enhanced delivery of Dox and cell killing effect. The *in vivo* study was done using SCID mice with xenografts of MiaPaCa-2. Animals were treated by IV injection with saline solution, free Dox, unloaded nanovalve-modified MSNs, nanovalve-modified MSNs loaded with Dox, and Tf-nanovalve-modified MSNs loaded with Dox. The average body weights of those treated mice without DOX were unchanged. The results of the hematology and serology examinations also showed the safety of these nanoparticles to the mice. The tumors in the control group and unloaded nanovalve-modified MSN group kept growing. However, significant tumor growth inhibition was found in the mice treated with Dox-loaded nanovalve-modified MSNs, showing the effective delivery of Dox by the nanoparticles inside the tumor. There was almost no difference in growth inhibition between targeted and untargeted particles, which may be explained by a protein corona that blocks the transferrin protein from being sensed by the Tf receptors of cancer cells [35].

β-CD rings and benzimidazole stalks

Xue, *et al.* [36] reported a different pH responsive pseudorotaxane nanovalve based on a benzimidazole stalk and a β-cyclodextrin (β-CD) ring, and studied its autonomous drug release *in vitro* (Figure 9). A series of benzimidazole derivates were tested, and methyl-1*H*-benzimidazole (MBI) was chosen as the stalk because of the pH range for protonation. It forms noncovalent bonding interactions with β-CD at pH 7.4, and protonates at lower pH (pH 6 or less) leading to weaker binding and release β-CD. THP-1 and KB-31 cell lines were chosen for *in vitro* study. After MBI was attached on the MSN surface, cargo was loaded followed by β-CD capping. Hoechst dye was first used to verify the delivery performance, and it showed little premature release at pH 7 and rapid release at pH 6 and lower. Then DOX was loaded for *in vitro* study. The release of DOX was slower compared to that of the dye and incomplete due to electrostatic interactions between the positively charged DOX and the negatively charged pore walls of the MSNs. To mitigate these charge effects, positively charged ammonium groups were co-condensed on the MSN, and rapid triggered release was observed. This system was tested in cell culture media to study the biological influence on the delivery system and it was fully functional under culture media conditions.
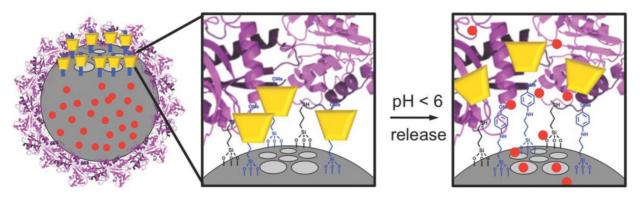

Figure 8. Depiction of the fully assembled Tf-nanovalve-modified MSN system. The operation of the aniline/α-CD valve was not inhibited by the Tf coating. Reprinted with permission from [34], copyright (2015) Small.
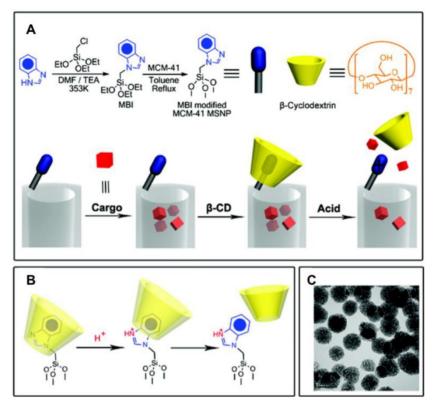
Figure 9. A. Steps of stalk synthesis, cargo loading, capping, and release. B. Cap dissociation from protonated stalk after pH decreases below 6. C. TEM image of the capped MSN. Reprinted with permission from [36], copyright (2010) J. Am. Chem. Soc.

Finally, the actions of the MSNs were studied *in vitro*. FITC-labeled MSN was first used to demonstrate that MSN was taken up by cells in acidic lysosomes. Using confocal microscopy, it was shown that more than 80% FITC-labeled MSN was colocalized with TRITC-labeled anti-LAMP-1 antibody labeled lysosomes in both cell lines. Then the release of Hoechst dye was studied in both cell lines. At 1 and 3 hours there was no release, but after 6 h, acidification caused the dye to be released to the nuclei of both THP-1 and KB-31. In the NH_4Cl treated cells, where the pH of lysosomes was increased to pH 6, the Hoechst staining was not found in nuclei. The release of DOX was studied in KB-31. After taken up by cell, the MSNs released DOX and led to apoptotic cell death. However, in the NH_4Cl treated cells where acidification was suppressed, little cell death was observed.

Pseudorotoxane nanovalves for treatment of infectious diseases

Two of the pH-activated cyclodextrin capped nanovalves described above, the one with the anilinoalkane stalk and the other with the benzimidazole stalk, were used to treat intracellular bacterial infectious disease. Mononuclear phagocytes, primarily monocytes and tissue macrophages, are known as professional phagocytes because of their reputation for avidly ingesting and killing bacteria. However, one class of pathogens, known as intracellular parasites, intentionally induces their uptake by macrophages with the aim of hijacking host cell machinery towards their own end – survival and intracellular replication. The two pseudorotaxane nanovalves were used to kill *Francisella tularensis* (Ft), the agent of tularemia. This bacterium is referred to by the US government as a Tier 1 Select Agent because of especially high concern that they may be intentionally employed in a bioterrorist attack.

Li *et al.* [37] optimized pH-responsive nanovalves functionalized MSNs to deliver moxifloxacin (MXF) for Ft infection treatment both *in vitro* and in *vivo* (Figure 10). Two pH-responsive nanovalves were chosen: one consisted of anilinoalkane (ANA) stalks and α-CD caps, and the other was composed of 1-methyl-1H-benzimidazole (MBI) and β-CD caps. Both stalks become protonated at pH 6 and lower, thus the caps dissociated and cargo released in lysosomes. The MSNs were optimized in the following aspects: charge of pore wall, efficiency of stalk attachment, concentration and pH of loading solution, loading duration and MSN washing after loading.

MSN uptake by macrophages was first tested *in vitro*. A large amount of uptaken rhodamine-labeled MSNs was observed in both the monocyte-derived

macrophages and the differentiated THP-1 cells. To investigate the efficacy in killing Ft, MXF loaded MSN with ANA/α-CD (MXF-MSN-ANA) or MBI/ β-CD (MXF-MSN-MBI) and control MSN without MXF loading were used to treat infected THP-1 for one day. Ft was killed by both MXF-MSN-ANA and MXF-MSN-MBI while the bacteria grew with control MSN or no treatment. Compared at the same concentration, MXF-MSN-MBI killed more Ft than MXF-MSN-ANA.

MXF-MSN-MBI was tested *in vivo*. Mice were infected with Ft and suffered severe weight loss without treatment. However, mice treated with MXF-MSN maintained their weight. Also, without treatment, Ft grew rapidly, but intravenously administered MXF-MSN-MBI decreased the number of bacteria in lung by 4.0 logs. MXF-MSN-MBI was more effective than 2 to 4 times higher dose of free MXF killing Ft in lung.

β-CD rings and azobenzene derivatives

Most of the pseudorotaxane nanovalves discussed up to this point were stimulated by pH changes that switched stalks from hydrophobic to hydrophilic and thus decreased the binding constants to the hydrophobic interiors of cyclodextrins. The pH changes from that of blood to that of lysosomes caused autonomous cargo release and the use of transducers such as photoacids enable light activation. A different way of releasing cyclodextrin and drugs involves molecular geometry changes and accompanying polarity changes.

Azobenzene derivatives undergo photo-induced reversible trans-cis isomerization when the molecules are irradiated with UV or blue light [38–40]. Azobenzene derivatives can be grafted on the interior pore walls of MSNs and the back-and-forth wagging motion in the pores can trap and release cargo molecules. This type of nanomachine has been called an impeller [41–44]. Azobenzene derivatives can also be grafted on the outside surface of MSNs and bind cyclodextrin when in the trans- conformation and dethread in the cis- conformation, serving as photosensitive gatekeepers, to control and regulate cargo release from MSNs. For example, Ferris *et al.* attached two types of azobenzene derivatives prepared from 4-(3-triethoxysilylpropylureido) azobenzene and (E)-4-((4-(benzylcarbamoyl)phenyl) diazenyl) benzoic acid to the outer surface of MSNs (Figure 11) [45]. Those azobenzene derivatives bind β-CD in their trans- form and then the β-CD caps were released when the azobenzene derivatives photoisomerize to the cis- conformation after irradiation with UV light. The authors showed that RhB was released after the UV light actuation.
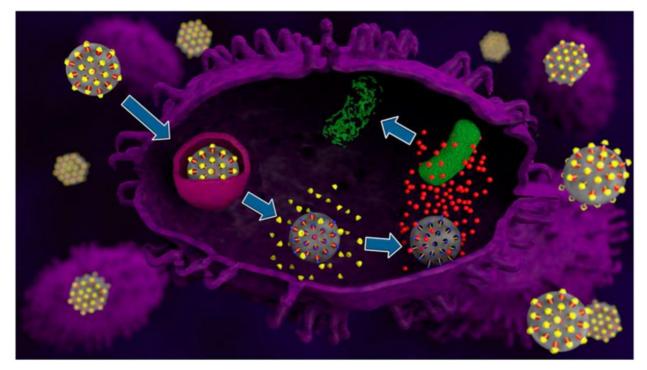

Figure 10. Moxifloxacin-loaded MSNs functionalized with pH-responsive capping system were uptaken into lysosomal compartments in a macrophage. The pH-responsive cap was opened and moxifloxacin was released to kill the intracellular *Francisella tularensis*. Reprinted with permission from [37], copyright (2015) ACS Nano.
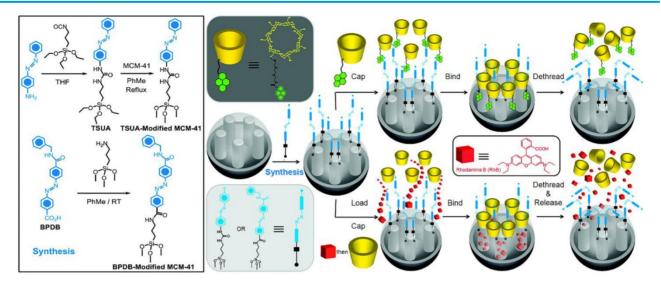
Figure 11. Synthesis of 4-(3-triethoxysilylpropylureido)azobenzene (TSUA)- and (E)-4-((4-(benzylcarbamoyl)phenyl)diazenyl) benzoic acid (BPDB)-modified MCM-41. Two approaches to the operation and function of the azobenzene-modified MCM-41 NPs carrying nanovalves. Py-β-CD or β-CD threads onto the trans-azobenzene stalks to seal the nanopores. Upon irradiation (351 nm), the isomerization of trans-to-cis azobenzene units leads to the dissociation of Py-β-CD or β-CD rings from the stalks, thus opening the gates to the nanopores and releasing the cargo. Reprinted with permission from [45], copyright (2009) J. Am. Chem. Soc.

Compared with UV light, red and near-infrared (NIR) light in the therapeutic window (600-1000 nm) are preferable for biomedical applications due to better tissue penetrability and decreased photodamage to biological systems. Tetra-ortho-methoxy-substituted azobenzene (mAzo) can undergo trans-to-cis isomerization when irradiated with red light. Wang *et al.* attached mAzo and β-CD on the surface of MSNs as the capping systems to control release of DOX by using red light (625 nm) (Figure 12) [46]. To show the photo-responsiveness of this capping systems in deep tissue, drug release was investigated by placing a piece of pork tissue (2 mm thick) between the light source and the sample. Although a lower release rate and amount were observed compared with that without tissue, red light irradiation at low power (60 mW/cm^2, 360 min) still induced DOX release (23%) after passing through the tissue.

Electrochemical and redox activation of pseudorotaxane valves

Khashab and coworkers [47] reported a ferrocene and β-CD/ cucurbit [7] uril (CB[7]) based nanovalve that was responsive to redox and pH changes (Figure 13). Ferrocenedicarboxylic acid was coupled to amine-functionalized surface of MSN, and RhB dye was loaded as the cargo. Then β-CD or CB[7] was capped by host-guest interaction. At pH 2, CB[7] was bound to protonated ferrocenedicarboxylic acid, and when pH increased to 10, ferrocene dianion was formed and the binding affinity to CB[7] was decreased. This mechanism was supported by NMR spectroscopy and cyclic voltammetry. The release

profile of CB[7] was tested: limited leakage was observed before trigger, and the emission intensity of the released RhB increased immediately after trigger. The β-CD cap was more sensitive to the electrochemical oxidation trigger and had minimal activation from pH modulation.

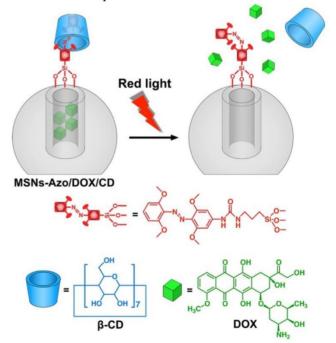**Figure 12.** Cartoon of the red-light-responsive drug delivery system constructed by MSNs modified with mAzo/β-CD supramolecular valves. Reprinted with permission from [46], copyright (2016) Langmuir.

Calix[n]arenes

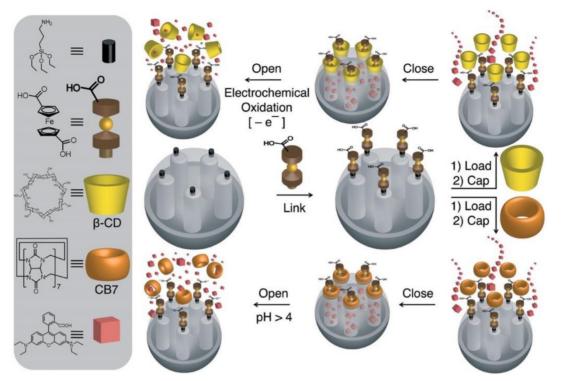A third type of macrocyclic rings in supramolecular chemistry, in addition to

Figure 13. Design and preparation of ferrocene-based mechanized nanoparticles, which operate under redox or pH control according to the nature of the ring (β-CD in the top route and CB7 in the bottom route) capping the pores. Reprinted with permission from [47], copyright (2009) European J. Org. Chem.

cyclodextrins and cucurbit[n]urils, are the calix[n]arenes. They are made up of phenol units linked by methylene bridges. Although calix[n]arenes have been incorporated with mesoporous silica materials, only a few studies have used calix[n]arenes as stimulus-responsive nanovalves for controlled cargo release compared with cyclodextrins and cucurbit[n]urils. Among different analogues of calix[n]arenes, sulfonato-calix[n]arenes (designated as SC[n]A) are water-soluble and have been reported to be biocompatible.

Calix[n]arenes rings and acetylcholine stalks

Yang *et al.* reported a supramolecular valve based on sulfonatocalix[4]arene (SC[4]A) that demonstrated NIR light-triggered cargo release (Figure 14) [48]. Mesoporous silica-coated gold nanorods (AuNR@MSNs) were synthesized followed by grafting acetylcholine stalks onto the nanoparticles. RhB as a model drug was loaded in the mesopores. SC[4]A was then added to encircle the stalks on the surface of AuNR@MSNs *via* host-guest complexation to form the supramolecular switches. Plasmonic heating generated from AuNR cores upon NIR light stimulation decreased the SC[4]A ring-stalk binding affinity, and thus dissociated the SC[4]A rings from the stalks and released the cargos. The release of RhB was monitored by UV-vis absorption spectroscopy. "Ladder" release profile generated by

using periodic ON/OFF NIR laser irradiation showed the ability to control the dose.

Figure 14. Schematic representation of SC[4]A-QAS nanovalves based on AuNR@MSN. The nanovalves can be operated by either NIR light irradiation or external heating to regulate the release of RhB. Reprinted with permission from [48], copyright (2014) Chem. Sci.

Crown ethers

Crown ethers have been used to construct stable complexes with alkali and transition-metal cations *via* electrostatic interactions [49]. The complexes can be

perturbed by pH and ultrasonic waves [50,51], where the changes in pH may weaken the electrostatic interactions and hydrogen bonding, and the gain of energy form ultrasound may lead to the dissociation of metal cations from crown ethers. These properties make the crown ether/metal cation complexes candidates for supramolecular nanovalves. By conjugating crown ethers onto the pores entry of MSNs, the loaded cargos can be entrapped in the presence of capping agents (*i.e.*, metal cations) and be released upon triggered by pH and ultrasonic waves.

Leung *et al.* developed Fe₃O₄@SiO₂ core−shell nanoparticles capped with crown ethers for ultrasound and pH-responsive drug release [52]. The core-shell structure was prepared by coating Fe_3O_4 nanoparticles with a mesoporous silica shell using modified hydrothermal sol−gel reactions. The mesoporous silica shell was functionalized with APTES and then coupled to dibenzo-crown ethers through amide linkages. Then DOX was loaded and the pores of the core−shell nanoparticles were capped with Na^+ and Cs^+ ions through the formation of complexes with the crown ethers on the outer surface. DOX controlled release was tested in PBS at pH 4 or pH 7.4. The results showed that DOX release was triggered at pH 4 in combination with ultrasound. This is because the pores were uncapped by lowering pH in the presence of ultrasound which broke up the interaction between the metal cations and crown ether's ethylene glycol chains. MTT assays confirmed that the crown ether/metal cation complexes capped nanoparticles were biocompatible to L929 cells (a murine aneuploidy fibrosarcoma cell line). Reasonable cellular uptake of the nanoparticles in L929 cells was observed from MRI analysis.
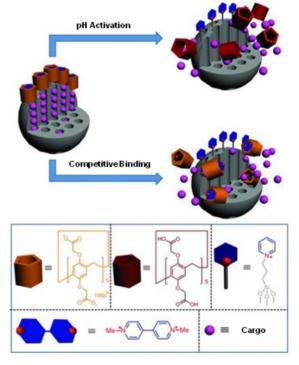
Pillararenes

Pillarenes are synthetic macrocycles that were first synthesized in 2008 and subsequently attracted attention in drug delivery research [53]. A supramolecular construct incorporated in an MSN based drug delivery system was reported by Sun, *et al.* in 2013 [54]. A pyridinium compound that is positively charged at neutral pH was attached to MSN surface as a stalk (Figure 15). Negatively charged carboxylatopillar[5]arene (CP[5]A) was used as a cap and held in place by the electrostatic attraction to the stalk. When the pH was decreased below 5, CP[5]A was protonated which weakened its interaction with stalk and led to uncapping. Methyl viologen salts can also trigger uncapping because of its higher binding affinity with CP[5]A.

Huang *et al.* utilized phosphonated pillar[5]arenes (PPA[5]) as capping agents in an MSN based drug delivery system [55]. Specific ion paring

between hydrated phosphonates on PPA[5] and quaternary ammoniums on stalks capped the pores tightly. When PPA[5] was protonated, the host-guest interaction between cap and stalk weakened, leading to cargo release. Competitive binding by Zn^{2+} ions also caused decapping and cargo release. Additionally, when gold nanorods (GNRs) were embedded inside MSNs and irradiated with near-infrared (NIR) radiation, the photothermal increase in temperature weakened host-guest interaction.

The PPA[5] gated GNR@MSNs were studied *in vitro* using human A549 lung carcinoma cell line. The empty particles showed no cytotoxicity. When the particles were loaded with DOX, cell apoptosis was observed and was increased with the NIR trigger due to the synergistic effect of photothermo-chemotherapy.

Figure 15. Diagram of pillar[5]arenes derivative based MSN drug delivery system. It can be triggered by both pH and competitive binding. Rhodamine B (RhB), calcein, and doxorubicin hydrochloride (DOX) were used as cargos. Reprinted with permission from [54], copyright (2013) Small.

Reversible rotaxane based nanovalves

Rotaxane supramolecular systems that can uncap and recap the pores of MSNs reversibly (without loss of the cap from the stalk) are discussed in this section. After assembling the complex formed by nanocap and stalk on the surface of the nanoparticle, the "closed" state of the stalk with the region of highest affinity brings the nanocap close enough to the particle surface to prevent cargo

leakage. The "open" state starts when binding between the nanocap and the stalk is no longer favorable, where the nanocap slides along the stalk away from the surface of the nanoparticle until reaching an end-terminating stopper group. The objective of putting the end-terminating stopper group is to prevent the nanocap from unthreading completely so that the above "closed" and "open" states can be switched reversibly. A variation on this theme is to position two binding sites on the stalk with the strongest binder nearest the pore opening. When the binding of the cap to the strong site is turned off, the ring slides to the weaker binding site and stops. When the strong binding is turned on again, the cap slides back. This motif resembles the action of a rotaxane but the blocking of cap release is caused by the second binding site and not a physical steric blocking group.

CB[6] rings and trisammonium stalks

Angelos *et al.* have designed a completely reversible valve based on CB[6] and trisammonium stalks (Figure 16) [56]. Propidium iodide (PI) cargo was loaded by soaking the stalk-attached nanoparticles in the PI solution overnight so that the dye molecules can diffuse into the empty nanopores. To complete the valve, CB[6] was added to the mixture to form an inclusion complex composed of the CB[6] rings and the trisammonium stalks. The beauty of this system is that it operates like a "dialed-in" clock system to selectively release the cargo at both low and high pH. At neutral pH, the two nitrogen atoms separated by four carbon atoms are protonated, therefore, through ion−dipole binding interactions between both portals of the macrocycle, the CB[6] ring is pulled down to sit close to and thus block the nanopores. When pH is low (~5), the anilinium nitrogen atom separated by six carbon atoms from the ammonium nitrogen is protonated thus moving the CB[6] ring to the distal hexamethylenediammonium station and releasing PI. The binding constant of CB[6] is strongest with nitrogens separated by the six carbons. At high pH (~10), all three nitrogen atoms on the stalk are deprotonated thus dethreading the CB[6] ring and releasing PI. These mechanized nanoparticles are highly dispersible in water, making this system a good candidate for the biological applications whose goal is to kill cells at both low and high pH.

α-CD rings and azobenzene derivatives

Tarn *et al.* developed two azobenzene-based rotaxane nanovalves with reversibility in response to blue light (403 nm) irradiation (Figure 17) [57]. These nanovalves were synthesized as follows. First,

p-nitrobenzoic acid was reacted with glucose to give 4,4'-azobenzenecarboxylic acid. Then, 4,4'-azobenzenecarboxylic acid was reacted with N-hydroxysucciminide to conjugate at one end with two adamantane-based molecules of different lengths, respectively. Next, the resulting azobenzene-containing molecules were complexed with α-CD to form the α-CD/azobenzene pseudorotaxanes. Finally, those pseudorotaxanes of different lengths were attached to aminopropyltriethoxysilane (APTES) modified-MSNs, yielding the ready-to-use nanocarriers. It is notable that the authors completed all the nanovalve attachment including stalks and nanocaps before loading cargos instead of *vice versa*. The method of loading cargos was by suspending the nanovalves in organic solvents under UV light irradiation to destabilize hydrophobic interactions between α-CD and the azobenzene moiety. To cap the pores after cargo loading, the particles were suspended in water in the dark to allow rebinding of the α-CD to azobenzene. Three fluorescent dyes with size between 1 and 2 nm, alizarin red S, PI, and Hoechst 33342, were chosen as the cargo molecules. The authors demonstrated that the two stalks of different lengths allowed the selective loading and release of those dyes based on the size. The adamantane functional group was selected as the stopper for two reasons: it is bulky enough (diameter of 0.5 nm) to prevent α-CD from unthreading; its binding affinity (binding constants of 100 M^{-1} [58]) with α-CD is lower than trans-azobenzene with α-CD so that competitive binding is limited. In this way, α-CD will either bind trans-azobenzene ("closed" state) or forms a metastable adamantane/α-CD state that holds the nanocap away from the pore openings ("open" state) when cis-azobenzene is formed by photoexcitation. The reversibility of the designed nanomachines was demonstrated by sequential fluorescence spectra. When the near-UV light was turned off, the fluorescence intensity leveled off until the stimulus was reapplied.

Inactive supramolecular systems

In addition to the supramolecular systems discussed above, there are other types of mechanisms involving bulky host-guest supramolecules that are not themselves serving as the active parts. These types of systems are called "inactive supramolecular systems". They typically use a bulky inclusion complex with a labile bond linked to the particle. The whole supermolecular complex is removed intact by bond cleavage through heat [59], photo-redox [60], or pH [61] at a location between the inclusion complex and nanoparticles.
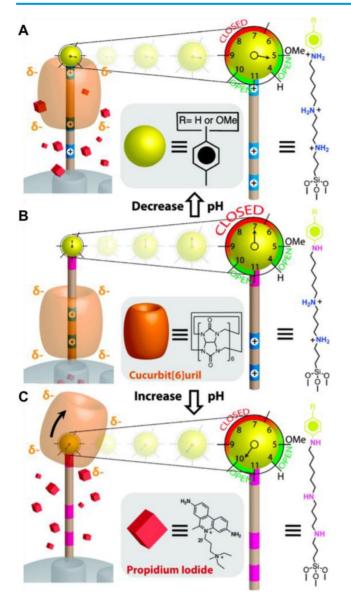
Figure 16. Design and pH-dependent operation of mechanized nanoparticles. (A) When pH is lowered such that the anilinium nitrogen atom is protonated, the CB[6] ring shuttles to the distal hexamethylenediammonium station, and PI is released. (B) At neutral pH, the CB[6] ring sits on the tetramethylenediammonium recognition unit, blocking the nanopores. (C) When the pH is raised, all of the nitrogen atoms on the stalk are deprotonated resulting in dethreading of the CB[6] ring. The system is designed such that the pH-response can be fine-tuned by changing the functional group R to modulate the pKa of the anilinium nitrogen atom. Reprinted with permission from [56], copyright (2009) J. Am. Chem. Soc.

Activation using thermal-sensitive bonds

Very recently, Chen *et al.* developed a β-CD-adamanatane cap held on to the superparamagnetic core@silica shell nanoparticles by a thermo labile bond on 4,4'-azobis(4-cyanovaleric acid) (ACVA) [62]. This bond was cleaved by the localized heat generated from the superparamagnetic core by oscillating magnetic field (OMF) actuation (Figure 18). The authors first demonstrated that the release amount of fluorescein cargos was adjustable by controlling the

OMF exposure time. *In vitro* drug release study was conducted to deliver DOX to PANC-1 cells. A positive correlation between the viability of the cells treated with DOX-loaded Mag@MSNs-AMA-CD and the OMF trigger time showed that dose control was achieved. Cells treated with nanoparticles without DOX less than 10 min of OMF exposure did not show any adverse effect, confirming that the heat generated from OMF interacting with the superparamagnetic core was not harmful to the cells.

Megagates and supramolecular amplifiers

A unique use of the admantane/β-CD interaction is formation of megagates over the large (6.5 nm) pores of SBA-15 silica. Xue, *et al.* designed and synthesized pH-responsive "weblike" megagates to cover the bigger pores with the goal of trapping cargo molecules (Figure 19) [61]. Two types of megagates, MG-1 and MG-2, were designed to cap and block larger and relatively smaller molecules, respectively. The extended structure of MG-1, which has a diameter of about 5.5 nm, was synthesized by linking a 1,3,5-triphenylbenzene core to three adamantane arms through triethylene glycol chains. MG-1 sufficiently prevents leakage of 4 nm dextran from the nanoparticle. To be able to reduce the gap between adamantane moieties for storing a smaller fluorescein disodium salt (FDS) cargo, hexaalkyne was chosen to be the core of MG-2 to generate a megagate with twice as many adamantane moieties as MG-1. To attach the megagate to the silica, ammine-modified β-CD stalks were grafted on the surface of SBA-15 through imine formation. Then, the adamantane arms form inclusion complexes with the β-CD and block the pores. FDS can diffuse freely out of the pore when a megagate is capped by MG-1, while dextran can only escape from the pore when the gate is opened due to the cleavage of imine bonds in the stalks at low pH.

Xue, *et al.* employed this megagate system to construct an enzyme-encapsulated MSN based chemical amplifier (Figure 20) [63]. In this study, the pH-responsive MG-2 enables substrate size-selectivity and thus controls the substrate access toward the encapsulated porcine liver esterase (PLE) in the MSN pores. PLE substrates 4-acetozycinnamic acid (ACA) and 5-carboxy-fluorescein diacetate (CFDA) were chosen due to their different sizes. The CFDA molecules are too big to pass through the megagate; only the small ACA analytes are able to diffuse in and out of the gaps between the adamantane moieties. ACA analytes undergo hydrolysis reactions after they interact with the hydrolase enzymes in the pores, generating acetic acid to actuate the megagate and allowing CFDA molecules to diffuse into the pore.

Hydrolysis of CFDA produces a fluorescent product. The catalytic amplification process then occurs due to the subsequent gate opening of the neighboring pores resulted from the additional hydrolysis of CFDA, and the process is monitored by increase in the fluorescence signal.
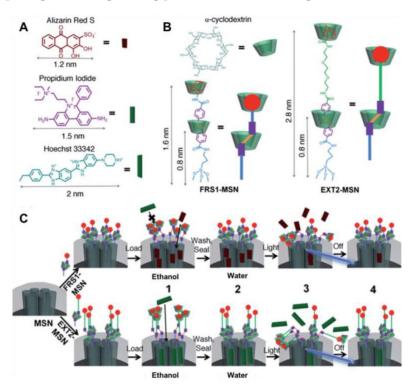

Figure 17. (A) Size illustration of various cargo molecules and (B) azobenzene stalks FRS1-MSN and EXT2-MSN. Because of the shorter stalk length, FRS1-MSN is limited to loading cargo molecules <2 nm. Hoechst 33342 and propidium iodide dyes remain excluded from FRS1-MSN as a result of their size. However, EXT2-MSN is observed to load all three of the listed fluorophores. (C) Schematic illustration of the fully assembled rotaxane nanovalve and operation. (1) After synthesis, the nanovalves are suspended in an organic solvent, which destabilizes hydrophobic interactions between the α-cyclodextrin and azobenzene moiety and allows for cargo loading. (2) Upon solvent exchange to water, rebinding of the cyclodextrin to azobenzene seals in the loaded cargo. (3) Irradiation with light induces isomerization to cis-azobenzene, forcing cyclodextrin to move to the end of the stalk, and allowing cargo to release. (4) Upon removal of the light stimulus, thermal relaxation of cis-azobenzene to its more stable trans isomer allows rebinding of the cyclodextrin and seals in the remaining cargo. Reprinted with permission from [57], copyright (2014) Nanoscale.
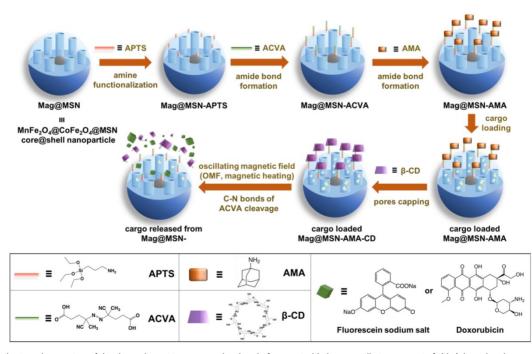

Figure 18. Synthesis and operation of the thermal-sensitive supramolecular platform activable by an oscillating magnetic field. Adapted with permission from [62], copyright (2019) ACS Nano.
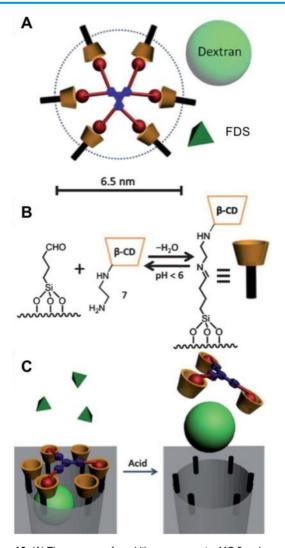
Figure 19. (A) The structure of a weblike megagate using MG-2 as the capping molecule. The relative sizes of the pore (dashed circle), the dextran cargo (the light green ball), and the smaller FDS cargo (the dark green pyramid) are shown. (B) Schematic representation of the cyclodextrin attachment onto the silica modified with aldehyde through imine formation. (C) The capping of megagate by MG-1 prevents the dextran from escaping, while FDS can freely diffuse out from the pore. Addition of acid allows the release of dextran. Reprinted with permission from [61], copyright (2012) Nanoscale.

Supramolecular snap-tops for stimuli responsive cargo delivery

A "snap-top" rotaxane is a supramolecule composed of a cyclic molecule on a stalk and a large "stopper" molecule attached to the end of the stalk to keep the cyclic molecule in place. The closed system is snapped open when the bulky stopper is removed thus allowing the cyclic molecule to move away from the pore. Patel *et al.* reported an enzyme-responsive snap-top nanovalve based on [2]rotaxane and α-CD (Figure 21) [64]. MSNs were first modified with APTES to introduce amine groups which were then alkylated with tri(ethylene glycol)monoazide monotosylate units. Next, the cargo loading step was

performed followed by the incubation with α-CD at 5°C for 24 h. At low temperature, α-CD threaded onto the tri(ethylene glycol) chains and effectively blocked the nanopores. The azide terminals of the cargo-loaded particles were then attached to adamantyl ester stopper molecules through Cu(I)-catalyzed azide-alkyne "click"cycloaddition. In this design, porcine liver esterase (PLE) catalyzed hydrolysis of the adamantyl ester stopper, allowing α-CD to dethread and release the cargo molecules from the pores. RhB was used as a model drug and the result from luminescence spectroscopy showed that rhodamine B was released only after adding PLE.

Ambrogio *et al.* reported another snap-top system in which stalks with disulfide bonds were encircled by CB[6] or α-CD rings and bulky adamantly groups at the terminal acted as the stoppers (Figure 22) [65]. The stalks were grafted onto MSNs through the reaction between azide-terminated diethylene glycol monotosylates and amino groups of APTES on the surface of MSNs. Then, nanoparticles were loaded with RhB followed by adding either CB[6] or α-CD to thread the stalks. The entire snap-top system was completed by click chemistry between the azide groups at the end of the stalks with propargyl ethers that contained disulfide linkages and bulky adamantly groups at the end. The two snap-top systems showed no leakage but released rhodamine B upon the addition of dithiothreitol (DTT) and 2-mercaptoethanol (ME) which reduced the disulfide bonds, removed the adamantly stoppers, and thus uncapped the pores of the CB[6] or α-CD-capped nanoparticles, respectively.

Another example of supramolecular snap-tops was designed by He *et al.* (Figure 23) [66]. In this design, an alkoxysilane and α-CD was also used as a stalk and a nanocap, and then serial peptide sequences were attached as the stopper molecule. The stopper, Gly-Phe-Leu-Gly (GFLG), can be hydrolyzed by cathepsin B, which is an overexpressed protease in various tumors. Almost 60% and 80% of the loaded DOX was released from the nanoparticles in the presence of cathepsin B at pH 7.4 and 5.0, respectively. Cervical cancer cells (HeLa) and a normal cell line of African green monkey SV40-transformed kidney fibroblast cells (COS7) were used to evaluate the targeting and drug release ability of DOX-loaded MSN-GFLGR$_7$RGDS/α-CD nanoparticles. These nanoparticles were shown not only to be efficiently taken up by tumor cells *via* integrins receptor-mediated targeting, but also can specifically release DOX into tumor cells *via* enzymatic digestion of GFLG peptide.
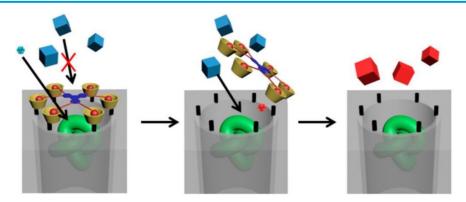
Figure 20. Schematic representation of the self-amplifying chemical sensing process. The megagate selectively allows only the small analyte molecule (blue ball) to diffuse into the pore to actuate megagate. Upon the opening of the gate, the substrate (blue cubes) is able to access the enzyme to initiate a catalytic production of fluorescent molecules. Reprinted with permission from [63], copyright (2013) J. Am. Chem. Soc.
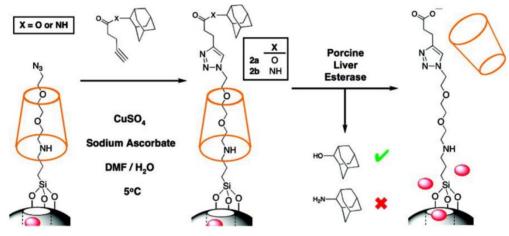

Figure 21. Synthesis and activation of an enzyme-responsive snap-top system. Reprinted with permission from [64], copyright (2008) J. Am. Chem. Soc.
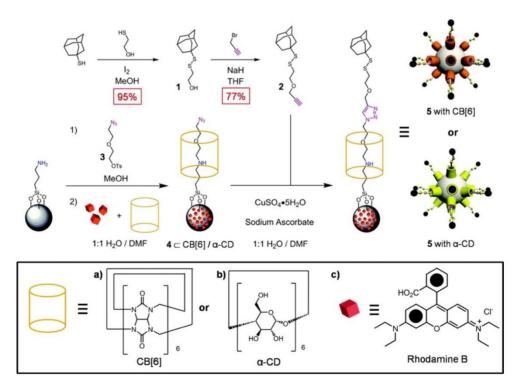

Figure 22. Synthesis of the alkyne-terminated stopper and assembly of disulfide-based snap-top nanocarriers. The nanocarriers studied utilize CB[6] or α-CD as the capping agent and Rhodamine B as the cargo. Reprinted with permission from [65], copyright (2010) Org. Lett.
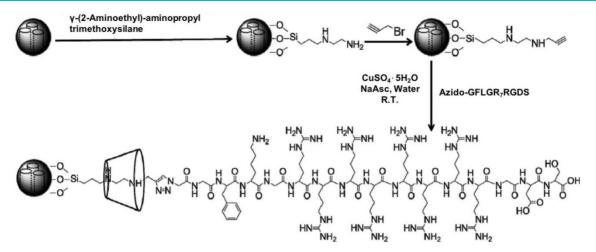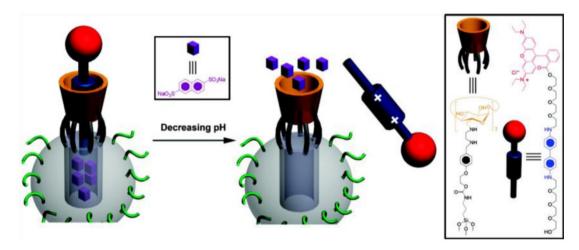
Figure 23. Preparation and structure of MSN-GFLGR$_7$RGDS/α-CD snap-top. Reprinted with permission from [66], copyright (2015) ACS Appl. Mater. Interfaces.

Figure 24. Schematic illustration of rhodamine B/benzidine inserted in the cavity of β-CD and acting like a piston due to the pH change, which makes cargo release. An ideal mode is to have one nanopore functionalized with one β-CD ring, as shown in the figure. Reprinted with permission from [67], copyright (2010) J. Am. Chem. Soc.

Nanopistons and their use as size-selective caps

A supramolecular nanopiston can serve as a gate to control cargo release. The piston consists of a molecule that moves in or out of a cavity provided by a ring (such as β-CD) that is immobilized around the opening of the pores. In this section, combination of a nanopiston with an inactive supramolecular system that allows sequential release of small molecules by the first stimulus and larger molecules by a second different stimulus is discussed.

Zhao *et al.* designed and fabricated a MSN-based nanopiston (Figure 24) [67]. This pH-mediated dual cargo delivery system consisted of β-CD which is covalently linked around the portal of the nanopores of MSNs and a RhB/benzidine compound that is inserted into the cavity of β-CD and moves in and out like a piston. It can control the trapping and release of the cargo molecules in response to pH changes. At neutral conditions, small cargos are trapped in the pore of MSNs and the RhB/benzidine plug blocks the β-CD gate tightly. As the pH value of the system decreased from 7 to 4, the protonated RhB/benzidine plug left the cavities of β-CDs and the small cargo was released by diffusing through the cavities of β-CD.

A similar design can be used for dual-cargo delivery that can sequentially deliver two different sizes of cargos on-command. It has the potential to achieve combination drug therapy. Wang *et al.* functionalized MSN surfaces with β-CD, which served as a gate to store large Hoechst 33342 molecules (Figure 25) [68]. The second smaller cargo, p-coumaric acid (CA), was loaded by diffusing it through the cavities of the β-CD into the pores of MSNs. Methyl orange (MO) was then added into the system to form a complex with the β-CD and plug the β-CD rings. Upon lowering the pH to 3.5, the formation constant between β-CD and MO decreased. The removal of the protonated MO molecules from

the β-CD cavities was followed by the release of the small CA cargo while the larger Hoechst 33342 were still blocked by the β-CD rings. Release of Hoechst 33342 was then triggered by introducing a reducing agent 2-mercaptoethanol that cleaved the disulfide bonds that linked the β-CD rings covalently onto the MSN surfaces. Removal of the β-CD rings released Hoechst 33342.

Summary

In keeping with the theme of this special issue of Theranostics, this review focused on supramolecular systems that carry out on-command, stimulated drug delivery. The review emphasized the mesoporous silica nanoparticles (MSNs) that have demonstrated efficacy *in vitro* and *in vivo*. There are of course very many other capping methods in addition to pseudorotaxanes and rotaxanes, and also many different types of nanoparticles have been studied [53,69–74]. Mesoporous silica forms a type of "hard" inorganic particle that is structurally stable for drug delivery [75,76]. For biomedical applications other important types of hard nanoparticles include those made from amorphous silica, gold, iron oxide, quantum dots and nanodiamonds [77–81]. Important types of "soft" nanomaterials include liposomes (the most successful in biomedical applications to date), polymers and dendrimers. Hybrid organic/inorganic particles have also been examined; particles made from organosilanes and lipid bilayer-coated silica are examples closely related to those discussed in this review. Many innovative capping systems on nanoparticles have also been used including thermal- and pH-sensitive polymers, and DNA to name a few. Supramolecular capping systems are fascinating, versatile, highly controllable, reversible, and biologically compatible. As is the case with other drug delivery systems, it is a long and costly road to clinical trials and eventual use in the clinic [82], but all of the above properties make supramolecular capping systems on mesoporous silica nanoparticles worthy of the attention that they are being given. Because of the importance of the biomedical applications, imaginative chemists, biologists, medical doctors, physicists and engineers will develop innovative new functional and controllable nanomaterials that will eventually advance to the clinic and help mankind.
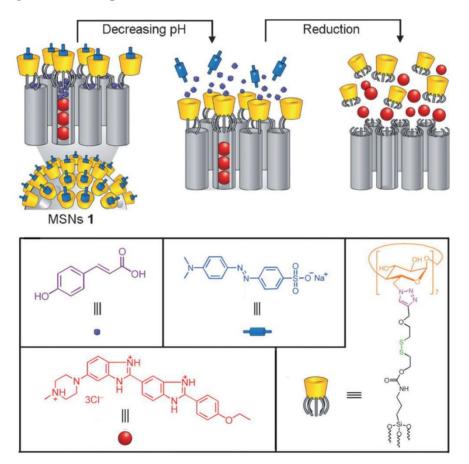

Figure 25. Schematic illustration of the dual-cargo release process. The first cargo release is achieved by lowering of pH and is followed by the second cargo release triggered by the presence of the reducing agent mercaptoethanol. Reprinted with permission from [68], copyright (2012) Angew. Chemie - Int. Ed.

Acknowledgments

Competing Interests

The authors have declared that no competing interest exists.

References

(1) Brinker CJ, Scherer GW. Sol-gel science the physics and chemistry of sol-gel processing. San Diego, USA: Academic Press; 1990.

(2) Stoddart JF. Mechanically interlocked molecules (MIMs)-molecular shuttles, switches, and machines (Nobel Lecture). Angew Chem Int Ed. 2017; 56: 11094-125.

(3) Dunn B, Miller JM, Dave BC, Valentine JS, Zink JI. Strategies for encapsulating biomolecules in sol-gel matrices. Acta Mater. 1998; 46: 737-41.

(4) Dave BC, Soyez H, Miller JM, Dunn B, Valentine JS, Zink JI. Synthesis of protein-doped sol-gel SiO₂ thin films: evidence for rotational mobility of encapsulated cytochrome c. Chem Mater. 1995; 7: 1431-4.

(5) Chung KE, Lan EH, Davidson MS, Dunn BS, Valentine JS, Zink JI. Measurement of dissolved oxygen in water using glass-encapsulated myoglobin. Anal Chem. 1995; 67: 1505-9.

(6) Miller JM, Dunn B, Valentine JS, Zink JI. Synthesis conditions for encapsulating cytochrome c and catalase in SiO₂ sol-gel materials. J Non-Cryst Solids 1996; 202: 279-89.

(7) Huang MH, Dunn BS, Zink JI. In situ luminescence probing of the chemical and structural changes during formation of dip-coated lamellar phase sodium dodecyl sulfate sol-gel thin films. J Am Chem Soc. 2000; 122: 3739-45.

(8) Nishida F, McKiernan JM, Dunn BS, Zink JI, Brinker CJ, Hurd AJ. In situ fluorescence probing of the chemical changes during sol–gel thin film formation. J Am Ceram Soc. 1995; 78: 1640-48.

(9) Klichko Y, Liong M, Choi E, Angelos S, Nel AE, Stoddart JF, et al. Mesostructured silica for optical functionality, nanomachines, and drug delivery. J Am Ceram Soc. 2009; 92: 2-10.

(10) Chiola V, Ritsko JE, Vanderpool CD. Process for producing low-bulk density silica. U.S. Patent. 1971; 3: 556-725.

(11) Lindén M. Biodistribution and excretion of intravenously injected mesoporous silica nanoparticles: implications for drug delivery efficiency and safety. In: Tamanoi F, Ed. The Enzymes. Oxford, UK: Elsevier; 2018: 155-80.

(12) Croissant JG, Brinker CJ. Biodegradable silica-based nanoparticles: dissolution kinetics and selective bond cleavage. In: Tamanoi F, Ed. The Enzymes. Oxford, UK: Elsevier; 2018: 181-214.

(13) Chia S, Cao J, Stoddart JF, Zink JI. Working supramolecular machines trapped in glass and mounted on a film surface. Angew Chem Int Ed. 2001; 40: 2447-51.

(14) Hernandez R, Tseng HR, Wong JW, Stoddart JF, Zink JI. An operational supramolecular nanovalve. J Am Chem Soc. 2004; 126: 3370-1.

(15) Flood AH, Liu Y, Tseng HR, Zink JI, Stoddart JF, Celestre PC, et al. A reversible molecular valve. Proc Natl Acad Sci. 2005; 102: 10029-34.

(16) Nguyen TD, Liu Y, Saha S, Leung KCF, Stoddart JF, Zink JI. Design and optimization of molecular nanovalves based on redox-switchable bistable rotaxanes. J Am Chem Soc. 2007; 129: 626-34.

(17) Saha S, Johansson E, Flood AH, Tseng HR, Zink JI, Stoddart JF. A photoactive molecular triad as a nanoscale power supply for a supramolecular machine. Chem Eur J. 2005; 11: 6846-58.

(18) Nguyen TD, Leung, KCF, Liong M, Liu Y, Stoddart JF, Zink JI. Versatile supramolecular nanovalves reconfigured for light activation. Adv Funct Mater. 2007; 17: 2101-10.

(19) Ambrogio MW, Thomas CR, Zhao YL, Zink JI, Stoddart JF. Mechanized silica nanoparticles: a new frontier in theranostic nanomedicine. Acc Chem Res. 2011; 44: 903-13.

(20) Lagona J, Mukhopadhyay P, Chakrabarti S, Isaacs L. The cucurbit[n]uril family. Angew Chem Int Ed. 2005; 44: 4844-70.

(21) Freeman WA, Mock WL, Shih NY. Cucurbituril. J Am Chem Soc. 1981; 103: 7367-8.

(22) Márquez C, Hudgins RR, Nau WM. Mechanism of host-guest complexation by cucurbituril. J Am Chem Soc. 2004; 126: 5806-16.

(23) Angelos S, Yang YW, Patel K, Stoddart JF, Zink JI. pH-responsive supramolecular nanovalves based on cucurbit[6]uril pseudorotaxanes. Angew Chem Int Ed. 2008; 47: 2222-6.

(24) Khashab NM, Belowich ME, Trabolsi A, Friedman DC, Valente C, Lau Y, et al. pH-responsive mechanised nanoparticles gated by semirotaxanes. Chem Commun. 2009; 5371-3.

(25) Thomas CR, Ferris DP, Lee JH, Choi E, Cho MH, Kim ES, et al. Noninvasive remote-controlled release of drug molecules in vitro using magnetic actuation of mechanized nanoparticles. J Am Chem Soc. 2010; 132: 10623-5.

(26) Croissant J, Zink JI. Nanovalve-controlled cargo release activated by plasmonic heating. J Am Chem Soc. 2012; 134: 7628-31.

(27) Kim K, Selvapalam N, Ko YH, Park KM, Kim D, Kim J. Functionalized cucurbiturils and their applications. Chem Soc Rev. 2007; 36: 267-79.

(28) Nau WM, Ghale G, Hennig A, Bakirci H, Bailey DM. Substrate-selective supramolecular tandem assays: monitoring enzyme inhibition of arginase and diamine oxidase by fluorescent dye displacement from calixarene and cucurbituril macrocycles. J Am Chem Soc. 2009; 131: 11558-70.

(29) Kim Y, Ko YH, Jung M, Selvapalam N, Kim K. A new photo-switchable "on-off" host-guest system. Photochem Photobiol Sci. 2011; 10: 1415-9.

(30) Sun YL, Yang BJ, Zhang SXA, Yang YW. Cucurbit[7]uril pseudorotaxane-based photoresponsive supramolecular nanovalve. Chem Eur J. 2012; 18: 9212-6.

(31) Du L, Liao S, Khatib HA, Stoddart JF, Zink JI. Controlled-access hollow mechanized silica nanocontainers. J Am Chem Soc. 2009; 131: 15136-42.

(32) Dong J, Xue M, Zink JI. Functioning of nanovalves on polymer coated mesoporous silica nanoparticles. Nanoscale. 2013; 5: 10300-6.

(33) Guardado-Alvarez TM, Russell MM, Zink JI. Nanovalve activation by surface-attached photoacids. Chem Commun. 2014; 50: 8388-90.

(34) Hwang AA, Lu J, Tamanoi F, Zink JI. Functional nanovalves on protein-coated nanoparticles for in vitro and In vivo controlled drug delivery. Small. 2015; 11: 319-28.

(35) Salvati A, Pitek AS, Monopoli MP, Prapainop K, Bombelli FB, Hristov DR, et al. Transferrin-functionalized nanoparticles lose their targeting capabilities when a biomolecule corona adsorbs on the surface. Nat Nanotechnol. 2013; 8: 137-43.

(36) Meng H, Xue M, Xia T, Zhao YL, Tamanoi F, Stoddart JF, et al. Autonomous in vitro anticancer drug release from mesoporous silica nanoparticles by pH-sensitive nanovalves. J Am Chem Soc. 2010; 132: 12690-7.

(37) Li Z, Clemens DL, Lee BY, Dillon BJ, Horwitz MA, Zink JI. Mesoporous silica nanoparticles with pH-sensitive nanovalves for delivery of moxifloxacin provide improved treatment of lethal pneumonic tularemia. ACS Nano. 2015; 9: 10778-89.

(38) Yoshida N, Seiyama A, Fujimoto M. Stability and structure of the inclusion complexes of alkyl-substituted hydroxyphenylazo derivatives of sulfanilic acid with alpha-cyclodextrin and beta-cyclodextrin. J Phys Chem. 1990; 94: 4254-9.

(39) Bortolus P, Monti S. Cis .Dblharw. Trans photoisomerization of azobenzene-cyclodextrin inclusion complexes. J Phys Chem. 1987; 91: 5046-50.

(40) Inoue Y, Kuad P, Okumura Y, Takashima Y, Yamaguchi H, Harada A. Thermal and photochemical switching of conformation of poly(ethylene glycol)-substituted cyclodextrin with an azobenzene group at the chain end. J Am Chem Soc. 2007; 129: 6396-7.

(41) Zhu Y, Fujiwara M. Installing dynamic molecular photomechanics in mesopores: a multifunctional controlled-release nanosystem. Angew Chem Int Ed. 2007; 46: 2241-4.

(42) Angelos S, Choi E, Vögtle F, De Cola L, Zink JI. Photo-driven expulsion of molecules from mesostructured silica nanoparticles. J Phys Chem C. 2007; 111: 6589-92.

(43) Lu J, Choi E, Tamanoi F, Zink JI. Light-activated nanoimpeller-controlled drug release in cancer cells. Small. 2008; 4: 421-6.

(44) Lau YA, Henderson BL, Lu J, Ferris DP, Tamanoi F, Zink JI. Continuous spectroscopic measurements of photo-stimulated release of molecules by nanomachines in a single living cell. Nanoscale. 2012; 4: 3482-9.

(45) Ferris DP, Zhao YL, Khashab NM, Khatib HA, Stoddart JF, Zink JI. Light-operated mechanized nanoparticles. J Am Chem Soc. 2009; 131: 1686-8.

(46) Wang D, Wu S. Red-light-responsive supramolecular valves for photocontrolled drug release from mesoporous nanoparticles. Langmuir. 2016; 32: 632-6.

(47) Khashab NM, Trabolsi A, Lau YA, Ambrogio MW, Friedman DC, Khatib HA, et al. Redox- and pH-controlled mechanized nanoparticles. Eur J Org Chem. 2009; 1669-73.

(48) Li H, Tan LL, Jia P, Li QL, Sun YL, Zhang J, et al. Near-infrared light-responsive supramolecular nanovalve based on mesoporous silica-coated gold nanorods. Chem Sci. 2014; 5: 2804-8.

(49) Gokel GW, Leevy WM, Weber ME. Crown Ethers: Sensors for ions and molecular scaffolds for materials and biological models. Chem Rev. 2004; 104: 2723-50.

(50) Wu Z, Ondruschka B, Stark A. Ultrasonic cleavage of thioethers. J Phys Chem A. 2005; 109: 3762-66.

(51) Cai Y, Pan H, Xu R, Hu Q, Li N, Tang R. Ultrasonic controlled morphology transformation of hollow calcium phosphate nanospheres: a smart and biocompatible drug release system. Chem Mater. 2007; 19: 3081-83.

(52) Lee SF, Zhu XM, Wang YX J, Xuan SH, You Q, Chan WH, et al. Ultrasound, pH, and magnetically responsive crown-ether-coated core/shell nanoparticles as drug encapsulation and release systems. ACS Appl Mater Interfaces. 2013; 5: 1566-74.

(53) Song N, Yang YW. Molecular and supramolecular switches on mesoporous silica nanoparticles. Chem Soc Rev. 2015; 44: 3474-504.

(54) Sun YL, Yang YW, Chen DX, Wang G, Zhou Y, Wang CY, et al. Mechanized silica nanoparticles based on pillar[5]arenes for on-command cargo release. Small. 2013; 9: 3224-9.

(55) Huang X, Wu S, Ke X, Li X, Du X. Phosphonated pillar[5]arene-valved mesoporous silica drug delivery systems. ACS Appl Mater Interfaces. 2017; 9: 19638-45.

(56) Angelos S, Khashab NM, Yang YW, Trabolsi A, Khatib HA, Stoddart JF, et al. pH clock-operated mechanized nanoparticles. J Am Chem Soc. 2009; 131: 12912-4.

(57) Tarn D, Ferris DP, Barnes JC, Ambrogio MW, Stoddart JF, Zink JI. A reversible light-operated nanovalve on mesoporous silica nanoparticles. Nanoscale. 2014; 6: 3335-43.

(58) Falvey P, Lim CW, Darcy R, Revermann T, Karst U, Giesbers M, et al. Bilayer vesicles of amphiphilic cyclodextrins: host membranes that recognize guest molecules. Chem Eur J. 2005; 11: 1171-80.

(59) Rühle B, Datz S, Argyo C, Bein T, Zink JI. A molecular nanocap activated by superparamagnetic heating for externally stimulated cargo release. Chem Commun. 2016; 52: 1843-6.

(60) Guardado-Alvarez TM, Devi LS, Vabre JM, Pecorelli TA, Schwartz BJ, Durand JO, et al. Photo-redox activated drug delivery systems operating under two photon excitation in the near-IR. Nanoscale. 2014; 6: 4652-8.

(61) Xue M, Cao D, Stoddart JF, Zink JI. Size-selective pH-operated megagates on mesoporous silica materials. Nanoscale. 2012; 4: 7569-74.

(62) Chen W, Cheng CA, Zink JI. Spatial, temporal, and dose control of drug delivery using non-invasive magnetic stimulation. ACS Nano. 2019; 13: 1292-1308.

(63) Xue M, Zink JI. An enzymatic chemical amplifier based on mechanized nanoparticles. J Am Chem Soc. 2013; 135: 17659-62.

(64) Patel K, Angelos S, Dichtel WR, Coskun A, Yang YW, Zink JI, et al. Enzyme-responsive snap-top covered silica nanocontainers. J Am Chem Soc. 2008; 130: 2382-3.

(65) Ambrogio MW, Pecorelli TA, Patel K, Khashab NM, Trabolsi A, Khatib HA, et al. Snap-top nanocarriers. Org Lett. 2010; 12: 3304-7.

(66) Cheng YJ, Luo GF, Zhu JY, Xu XD, Zeng X, Cheng DB, et al. Enzyme-induced and tumor-targeted drug delivery system based on multifunctional mesoporous silica nanoparticles. ACS Appl Mater Interfaces. 2015; 7: 9078-87.

(67) Zhao YL, Li Z, Kabehie S, Botros YY, Stoddart JF, Zink JI. pH-operated nanopistons on the surfaces of mesoporous silica nanoparticles. J Am Chem Soc. 2010; 132: 13016-25.

(68) Wang C, Li Z, Cao D, Zhao YL, Gaines JW, Bozdemir OA, et al. Stimulated release of size-selected cargos in succession from mesoporous silica nanoparticles. Angew Chem Int Ed. 2012; 57: 5460-5.

(69) Aznar E, Oroval M, Pascual L, Murguía JR, Martínez-Máñez R, Sancenón F. Gated materials for on-command release of guest molecules. Chem Rev. 2016; 116: 561-718.

(70) Kumar N, Chen W, Cheng CA, Deng T, Wang R, Zink JI. Stimuli-responsive nanomachines and caps for drug delivery. In: Tamanoi F, Ed. The Enzymes. Oxford, UK: Elsevier; 2018: 31-65.

(71) Argyo C, Weiss V, Bräuchle C, Bein T. Multifunctional mesoporous silica nanoparticles as a universal platform for drug delivery. Chem Mater. 2014; 26: 435-51.

(72) Wen J, Yang K, Liu F, Li H, Xu Y, Sun S. Diverse gatekeepers for mesoporous silica nanoparticle based drug delivery systems. Chem Soc Rev. 2017; 46: 6024-45.

(73) Yang YW. Towards biocompatible nanovalves based on mesoporous silica nanoparticles. MedChemComm. 2011; 2: 1033-49.

(74) Coll C, Bernardos A, Martínez-Máñez R, Sancenón F. Gated silica mesoporous supports for controlled release and signaling applications. Acc Chem Res. 2013; 46: 339-49.

(75) Chen W, Cheng CA, Lee BY, Clemens DL, Huang WY, Horwitz MA, et al. A facile strategy enabling both high loading and high release amounts of the water-insoluble drug clofazimine using mesoporous silica nanoparticles. ACS Appl Mater Interfaces. 2018; 10: 31870-81.

(76) Zhao N, Lin X, Zhang Q, Ji Z, Xu FJ. Redox-triggered gatekeeper-enveloped starlike hollow silica nanoparticles for intelligent delivery systems. Small. 2015; 11: 6467-79.

(77) Wu TJ, Tzeng YK, Chang WW, Cheng CA, Kuo Y, Chien CH, et al. Tracking the engraftment and regenerative capabilities of transplanted lung stem cells using fluorescent nanodiamonds. Nat. Nanotechnol. 2013; 8: 682-9.

(78) Fang CY, Vaijayanthimala V, Cheng CA, Yeh SH, Chang CF, Li CL, et al. The exocytosis of fluorescent nanodiamond and its use as a long-term cell tracker. Small. 2011; 7: 3363-70.

(79) Hui YY, Cheng CA, Chen OY, Chang HC. Bioimaging and quantum sensing using NV centers in diamond nanoparticles. In Yang N, Jiang X, Pang DW, Eds. Carbon Nanoparticles and Nanostructures. Cham, Switzerland: Springer International Publishing; 2016: 109-37.

(80) Chen X, Zhang Q, Li J, Yang M, Zhao N, Xu FJ. Rattle-structured rough nanocapsules with in-situ-formed gold nanorod cores for complementary gene/chemo/photothermal therapy. ACS Nano. 2018; 12: 5646-56.

(81) Duan S, Yang Y, Zhang C, Zhao N, Xu FJ. NIR-responsive polycationic gatekeeper-cloaked hetero-nanoparticles for multimodal imaging-guided triple-combination therapy of cancer. Small. 2017; 13: 1603133.

(82) Faria M, Björnmalm M, Thurecht KJ, Kent SJ, Parton RG, Kavallaris M, et al. Minimum information reporting in bio‑nano experimental literature. Nat Nanotechnol. 2018; 13: 777-85.

Author biography

Jeffrey I. Zink is a Distinguished Professor of Chemistry and Biochemistry and Co-director of the Cancer Molecular Imaging, Nanotechnology and Theranostics Program at the Jonnson Comprehensive Cancer Center at UCLA. He received his PhD degree from the University of Illinois. He is the author of more than 500 publications and his current research interests include miultifunctional nanomaterials and theranostic applications.

Chi-An Cheng was born in Taipei, Taiwan. She received her B.S. and M.S. degrees in Chemistry from National Taiwan University and did her research under Professor Huan-Cheng Chang in Academia Sinica. She is currently pursuing her PhD at UCLA Bioengineering under the supervision of Prof. Jeffrey I. Zink. Her current research focuses on developing multifunctional mesoporous silica nanoparticles and magnetic nanoparticles for their theranostic applications.

Tian Deng graduated from Shandong University, China with a BS in Chemistry in 2016. She is currently pursuing her PhD under the supervision of Prof. Jeffrey I. Zink at UCLA. Her research focuses on thermo-responsive polymer functionalized MSN and its biomedical application.

Fang-Chu Lin obtained her bachelor's and master's degrees from UCLA. She is currently a Ph.D student under the supervision of Prof. Jeffrey I. Zink. Her current research focuses on the analysis of nanoscale drug delivery system and the development of MRI contrast agents.

Yao Cai obtained his PhD degree from University of Chinese Academy of Sciences. Dr. Cai is a postdoctoral fellow in the Institute of Geology and Geophysics, Chinese Academy of Sciences and is a visiting scholar in Prof. Jeffrey I. Zink's group. His current research focuses on building multifunctional nanoplatforms based on biomineralization-related proteins and mesoporous silica nanoparticles.